Green chemistry principles for the synthesis of antifungal active gum acacia-gold nanocomposite - natamycin (GA-AuNC–NT) against food spoilage fungal strain *Aspergillus ochraceopealiformis*

Karthik Raja namasivayam (biologiask@gmail.com)
Sathyabama Institute of Science and Technology https://orcid.org/0000-0003-2894-1905
Mohit Manohar
Sathyabama Institute of Science and Technology
Akil Knde
Sathyabama Institute of Science and Technology
K Samrat
M S Ramaiah Institute of Technology
RS Bharani
Sathyabama Institute of Science and Technology
C Jayapraksh
DRDO Defense Food Research Laboratory

Research Article

Keywords: Green chemistry, natamycin, Gum acacia, Gold nanocomposite, Aspergillus ochraceopealiformis, Antifungal, Biocompatibility

Posted Date: March 23rd, 2022

DOI: https://doi.org/10.21203/rs.3.rs-1338723/v1

Abstract

Evaluation of potential anti fungal activity of gum acacia -gold nanocomposite fabricated with food preservative agent natamycin (GA-AuNC–NT and its noteworthy release pattern, biocompatibility was prepared in this present investigation. GA-AuNC–NT was prepared by green science principles under *in vitro* condition and the synthesized nanocomposite was characterized by various characterisation techniques. Green science principles that adopted in this study reveals highly stable nano dimensional composite with significant antifungal activity. The antifungal activity was investigated against the fungal strain *Aspergillus ochraceopealiformis* isolated from spoiled, expired bread. The well diffusion assay, fungal hyphae fragmentation assay and spore germination inhibition assay were used to determine the antifungal activity of the synthesised nanocomposite. Potential antifungal activity of the synthesised nanocomposite was confirmed by recording zone of inhibition, high rate of hyphae fragmentation and marked spore germination inhibition against the tested fungal strain. The molecular mechanism of antifungal activity was studied by measuring oxidative stress marker genes like catalase (CAT), superoxide dismutase (SOD), peroxidase (POD) induction adopting quantitative real-time polymerase chain reaction (q RT-PCR). Among the various treatment, a notable reduction in all the tested marker genes expression was recorded in the nanocomposite treated fungal strain. Release profile studies using different solvents reveal sustained or controlled natamycin release at the increasing periods. The synthesised nanocomposite's high safety or biocompatibility was evaluated with the Wistar animal model by determining notable changes in behavioural, biochemical, haematological and histopathological parameters. The synthesised nanocomposite did not exhibit any undesirable changes in all the tested parameters confirming the marked biosafety or biocompatibility. The nanocomposite was coated on the bread packaging material. The effect of packaging on the proximate composition, antioxidative enzymes status, and fungal growth of bread samples incubated under the incubation period were studied. Fourier transform infrared spectroscopy (FTIR) and scanning electron microscopy (SEM) studies reveal that the nanocomposite was effectively coated on the packaging material without changing size, shape, and functional groups. No changes in the proximate composition and antioxidative enzymes of the packaged bread samples incubated under different incubation periods reveal the nanocomposite's marked safety. The complete absence of the fungal growth also indicates the uniqueness of the nanocomposite. The present finding implies that the synthesised nanocomposite can be used as an effective, safe food preservative agent against food spoilage fungal strains associated with a wide range of food products and suggest a green strategy for the increased shelf life of foods.

1. Introduction

Different food preservation strategies have been utilised in the food sector to protect the foods from various undesirable effects (Chaudhry et al., 2008). Rather than food processing methods, preservations strategies have been recognised as an important parameter in the food industry (Wu et al., 2017). Food preservation practices protect the foods from various undesirable oxidative and microbes mediated spoilage. Among the food preservation methods, chemicals based preservation technology plays a

crucial role in the prevention of spoilage, mainly microbial attack/ These selected chemical preservatives like the salt of ascorbic, sorbic, benzoic, propionic acids, sulphites of potassium, calcium inhibits, kills or slow down the metabolic activity of microbial pathogens which in turn enhance the shelf life. (Parada et al., 2017).

Metabolites derived from biological sources have been used as preservatives for a few decades due to their high efficacy, stability and biocompatibility. Bacteriocins are peptides or proteins with antimicrobial activity against closely related microorganisms (Namasivayam et al., 2016). The bacteriocins delivered by lactic acid bacteria are proved to inhibit or eliminate the growth of foodborne pathogens like *Listeria monocytogenes, clostridium perfringens, Bacillus cereus*, and *Staphylococcus aureus*. Bacteriocinogenic lactic acid bacteria isolated bacteriocins are totalled as safe additives (GRAS), useful to control pathogens' systematic development and spoil microorganisms in foods and feed. Bacteriocin production could be counted as an advantage for food and feed producers since, in adequate amounts, these peptides can inhibit or kill the pathogenic bacteria that contend for the same ecological niche or nutrient pool (Namasivayam et al., 2014). This role is maintained because many bacteriocins have a narrow host array and are expected to be most effective against related bacteria with nutritional demands for the same scarce resources (Du et al., 2009).

Natamycin is the only microbial-based antifungal antibiotic compound used for decades in the food industry, followed by Lactobacillus-based bacteriocin as a food preservative mainly to inhibit undesirable fungal growth in various food products. It can be employed in multiple ways as an aqueous suspension sprayed on the product. It is a polyene macrolide biological antifungal agent produced by fermentation of the bacterium *Streptomyces natalensis*. EFSA (European Food Safety Authority) considered that the proposed usage levels of natamycin are safe when used for the surface treatment for these sausages and cheese type food products (Pedersen, 1992). Pedersen (Leyva et al., 2017) used natamycin in culture medium to prevent fungal growth. Most countries approve natamycin on cheese as surface treatment, and its addition into other foods depends on legislation (de Boer and Stolk-Horsthuis, 1977; Aparicio et al., 1999). Natamycin's antifungal activity against diverse pathogenic fungal strains has reported that natamycin blocks fungal growth by binding to ergosterol specifically without permeabilising the membrane (Te Welscher et al., 2008; Delattin et al., 2014).

Molecular mechanisms of natamycin based antifungal activity against various fungal strains have been reported (Te Welscher et al., 2012; Lalitha et al., 2007). A study by Prajna Lalitha et al., (2008) and Xu et al., (2008) revealed the antifungal activity of natamycin against clinical isolates of fungal strains. Antifungal susceptibility testing under laboratory conditions against the fungal isolates demonstrated the high efficacy of natamycin (Brothers and Wyatt, 2000; Al-Hatmi et al., 2016; Rees et al., 2019). The effect of natamycin on fungal corneal ulcers has been reported by Abhishakth Gerhardt et al., (2019). Jiang et al., (2020) reported synergistic antifungal activity of other antifungal drugs with natamycin against *Fusarium* sp. Natamycin induced antifungal action against plant pathogenic fungal strain *Colletotrichum gloeosporioides* has been studied by Liu et al., (2019).

In recent years, nanotechnology has been the most dynamic research field. It can control and manipulate matter in the nano-size (Prakash et al., 2019). Nanomaterials are used for many functions because, at this scale, unique optical, magnetic, electrical, and other properties (Fernandes et al., 2020). Nanotechnology has also shown versatile applications in safety, toxicity and risk assessment in the fields of agriculture, food and the environment (Namasivayam et al., 2018). In addition, the concept of nanotechnology has paved the way in the processing and formulation of colourants, sensors, flavours, additives, preservatives and food supplements (Shahbazi and Shavisi, 2019).

The prime focus of nanotechnology in food processing involves the development of nanostructured food ingredients and additives. This category of nanofood was being developed with claims that they offer enhanced taste, texture and consistency, enhanced bioavailability and allow mixing of “incompatible” ingredients in the food matrix. Nanotechnology derived food packaging resources are the prime category of existing nanotechnology applications for the food sector. Polymer nanocomposites combined with metal or metal oxide nanoparticles have been developed for antimicrobial “active” packaging, abrasion resistance, UV absorption or forte. The nanomaterials used as UV absorbers such as titanium dioxide can avert UV degradation in plastics such as PS, polyethene (PE) and polyvinylchloride (PVC). The metal and metal oxide nanomaterials in general used are iron oxides (Fe_3O_4, Fe_2O_3), gold (Au), zinc oxide (ZnO), silica (SiO_2), alumina (Al_2O_3), silver (Ag), and titanium dioxide (TiO_2). Other semiconductor nanoparticles (e.g., cadmium telluride/gallium arsenide) have also been used to develop nanocomposites. Nanoencapsulation technologies can meet food industry challenges concerning the effective delivery of healthy functional ingredients and controlled release of flavour components (Mohammadi et al., 2015; Badawy et al., 2019). The main types of nanoencapsulation systems for food application are formed from accepted food ingredients like lipids, carbohydrates, and proteins in GRAS (generally regarded as safe materials) (Kiss, 2020).

Among the various nanomaterials used in the food sector, nanocomposites have gained more attention due to their high efficiency, biodegradability and biocompatibility (Akhavan et al., 2018). A report of diverse nanocomposites like poly(vinyl alcohol) / chitosan/Montmorillonite nanocomposite for food packaging application (Butnaru et al., 2016), polysaccharides- ZnO nanocomposites for fruits coating (Leyva Salas et al., 2017; Sagun-bella et al., 2013; Fahimi and Ghorbani, 2019; Ahmed et al., 2021). Chitosan-based diverse metal oxide nanocomposites and chitosan nanocomposites (Hooda et al., 2018; Masheane et al., 2016; Meghani et al., 2019; Shanmuga Priya et al., 2014; Kumar et al., 2019; Padmanabhan et al., 2018; Bhatta et al., 2012), gum nanocomposites would suggest utilising nanocomposites in the food sector for the enhanced shelf life without affecting nutritional values (Boskovic et al., 2019).

In this present study, gum acacia gold nanocomposite fabricated with natamycin synthesised via green technology principles was evaluated against potential antifungal activity against fungal strain *Aspergillus ochraceopealiformis* with spoiled, expired bread. Gold nanoparticles synthesised by chitosan-based reduction of gold (III) chloride were transformed into functional nanocomposite (GA-AuNC-NT) with gum acacia via an eco-friendly route. Thus obtained, the synthesised nanocomposite was characterised

by suitable analytical techniques to confirm structural, functional properties. Well diffusion assay, dual liquid assay and mycelial or hyphal breakage assay were used to determine antifungal activity against the tested fungal strain. The molecular mechanism of antifungal activity was studied by determining oxidative stress marker genes like catalase, superoxide dismutase and peroxidase adopting qRT-PCR. The control release profile of the natamycin from the synthesised nanocomposite using different solvents was also investigated. Biocompatibility of the nanocomposite was studied with the Wistar rat model by determining changes or abnormalities in behavioural, physiological, biochemical and histopathological parameters. The effect of nanocomposite packaging on the proximate composition, antioxidative enzymes status and fungal growth was also examined.

2. Materials And Methods

2.1. Reagents and chemicals

Gold (III) chloride and medium molecular weight chitosan with 75-85 % deacylation were obtained from Sigma Aldrich as received. Analytical grade of gum acacia was purchased from Ranken. Food grade natamycin was obtained from the Defence Food Research laboratory (DFRL), Mysuru (Mysore), India. The culture medium used for antifungal testing was purchased from Hi-Media (India).

2.2. Gold nanoparticles (AuNps) synthesis

Gold nanoparticles (AuNps) were synthesised with chitosan as a reducer or stabiliser by the modified method of Ding & Zhu, (2015). This method, known volume of gold (III) chloride (1.5 mL with 0.5 % final concentration), was added dropwise to 1 % chitosan solution suspended in a 0.1 % acetic acid-distilled water mixture under magnetic stirring. After stirring at ambient condition, the homogenised solution was heated at 80^{o}C in a water bath till the reaction mixture turned into ruby red colour. Conversion of reaction mixture into ruby red confirmed the synthesis of AuNps. The reaction mixture containing synthesised AuNps was centrifuged at 10,000 ×g for 15 min to remove unreacted precursor at ambient condition followed by resuspension in distilled water (Coman et al., 2015).

2.3. Preparation of gum acacia gold nanocomposite grafted Natamycin (GA-AuNC-NAT)

In a typical procedure of GA- 45AuNC-NAT synthesis, a known quantity of synthesised AuNps (2.0 mL) was deferred in 18 mL of 0.1 % gum acacia followed by dropwise addition of natamycin (5 mL of 0.1 %) under magnetic stirrer at ambient condition (39ºC). After stirring, the suspension was centrifuged at 10,000 ×g at ambient conditions. The collected pellet was washed with deionised water to remove the agglomerates and non-reactive substances. The washed pellet was lyophilised and used for further studies.

2.3.1. Characterisation

Suitable characterisation techniques studied structural and functional properties of the synthesised nanocomposite. Functional group interaction between AuNps and gum acacia, which transformed into highly stable functional nanocomposite, was analysed by UV- vis spectroscopy, Fourier transform infrared spectroscopy (FTIR), scanning electron microscopy, and atomic force microscopy (AFM). Sample preparation, processing and analysis were done by standard methods. Primary confirmation to determine the structural changes by UV –vis spectroscopy was done with a double beam UV vis spectrophotometer (Shimadzu-1800 spectrophotometer with 800-200 nm range). A potassium bromide (KBr) pelletised sample was analysed for recording FTIR spectrum (FT-IR8300). Scanning electron microscopy analysis was used to study size & shape or particle morphology. SEM micrograph of the processed sample was recorded using carl –Zeiss Supra 55. Determination of surface topology or topography was done by AFM analysis. AFM micrograph of the processed sample was taken with Ntegra Prima (contact mode). The X-ray diffraction (XRD) study used to determine crystallinity was done with Bruker XRD. Particle size distribution was analysed by Malvern (UK). Sample preparation was conducted by standard method. The thermogravimetric analysis was carried out with a thermal analyser (Netzsch, STA 409) over a temperature range of 20-55ºC and a heating rate of 0.25ºC/min under an air atmosphere.

2.4. Antifungal activity

Antifungal activity of the synthesised nanocomposite was evaluated against food spoilage fungal organisms associated with expired bread. Ten samples of bread, including five expired and five unexpired (still valid for consumption) obtained from the local supermarket, were used in this study. All the collected samples were brought to the laboratory for microbiological analysis.

2.4.1. Fungal strain isolation

The known quantity of the bread sample (10 g) that derived from the respective item was deferred in 90 mL of sterile distilled water followed by incubation at ambient condition for 15 min. 1 mL of the suspended sample was then serially diluted in 9 mL distilled water under aseptic condition followed by plating on sterile potato dextrose agar supplemented with chloramphenicol to prevent bacterial contamination. The inoculated fungal plates were incubated at 28ºC for 4 - 5 days. After the incubation period, the fungal colonies that grew on the plate were counted. The number of colonies was reported as colony-forming units/g (CFU/g). The pure culture of the fungi was maintained on the PDA slant. The fungal strain was identified based on morphological and molecular characteristics. Culture morphology on the plate broth substrate and aerial mycelia microscopic examination of fungal spores using lactophenol cotton blue staining. 18S RNA sequencing was used to identify the fungal organism. Genomic DNA isolated from the pure culture of the fungal strain was amplified with primers of ribosomal ITS region followed by a Determination of sequence similarities using BLAST sequence analysis (NCBI database). Based on the sequence similarities, the isolated fungal strain was *Aspergillus ochraceopealiformis*.

2.4.2. Growth inhibition assay

For well diffusion assay, the fungal inoculum (spore suspension) was obtained from PDA slant using sterile distilled water- tween 20 (0.1 %) mixture under aseptic condition. A known volume of fungal inoculum (0.1 mL) thus obtained was uniformly spread on the sterile PDA plate followed by different concentrations of nanocomposite (25, 50, 75 and 100 µg) into the wells made with sterile gel puncture. Inoculated plates were incubated at 28^{o}C for 72 h. The zone of inhibition was measured after the incubation period. Compare the efficacy; free natamycin, free gold nanoparticles, gum acacia were used. Three replicates were maintained for each treatment.

The following formula calculated the percentage of growth inhibition

$$\text{Growth inhibition (\%)} = \frac{\text{colony diameter in control- colony diameter in treatment}}{\text{colony diameter in control}} X100$$

Further confirmation on growth inhibition was conducted by liquid assay. In this method, sterile potato dextrose broth (PDB) was inoculated with 0.1 mL of fungal inoculum followed by adding different concentrations of nanocomposite (25, 50, 75 and 100 µg. Inoculated flasks were incubated at 28°C for 72 h under shaking conditions. After the incubation, the seeded flasks were filtered through crude filter paper. The collected biomass was transferred to the Petri plate containing a filter paper. The initial weight of the paper was recorded. The Petri dishes were kept in a hot air oven at 50°C for one hour, and the dry weight of the biomass was recorded. The growth inhibition was determined by the difference between the dry weight of biomass in the control and the respective treatment.

2.4.3. Fungal hyphal fragmentation or breakage assay

Further confirmation of antifungal activity was done by fungal hyphal fragmentation or breakage assay. Sterile molten PDA medium supplemented with nanocomposite was transferred to the clean, sterile glass slide as agar plug placed in the sterile Petri plate lined with moist filter paper. A tuft of fungal mycelia was gently placed on the agar plug, covered with a coverslip, followed by incubation at 28^{o}C for 72 h. After the incubation period, the slides were observed microscopically to record hyphal fragmentation or mycelial breakage. Three replicates and control were maintained. Fragmentation efficacy expressed in percentage was determined by measuring the differences in the number of fragmented fungal hyphae in control and treatment (Narendrakumar et al., 2018).

2. 4. 4. Spore germination inhibition assay

Sterile molten soft agar with nanocomposite was transferred to the cavity slide under aseptic conditions to solidify. After solidification, a tuft of fungal mycelia was gently placed. The preparation was transferred to the Petri plate lined with moist filter paper, incubated at 28ºC. Under a microscope, the spore germination was observed, and the data obtained was used to record the germination index (%).

2. 4. 4. Morphological changes

Nanocomposite induced changes in the morphology of fungal strain were studied by scanning electron microscopy (SEM). The biomass was processed by a standard method, and an SEM micrograph was taken using carl –Zeiss Supra 55.

2. 4. 5. Oxidative stress assay

Nanocomposite induced oxidative stress was studied by quantification of reactive oxygen species (ROS), antioxidative enzymes like catalase (CAT), superoxide dismutase (SOD), peroxidase (POD), lipid peroxidase (LPO), non-enzymatic antioxidant reduced glutathione (GSH) and biomarker expression pattern of CAT, SOD and POD by qRT-PCR. The fungal strain was cultured in a sterile PDB with different dosages NT, GA, AuNps and GA-AuNC-NT under shaking conditions at ambient temperature. The cultured broth was centrifuged (10,000 ×g), and the collected mycelia were used for further studies.

2. 4. 5. 1. ROS generation

Collected mycelia were washed with phosphate-buffered saline (PBS) three times. Washed mycelia were mixed with known H2DCFH-DA (40mmol/L) volume followed by incubation at the dark condition at 28°C. ROS generation was quantified using a fluorescent spectrophotometer (Fluoromax-4, Japan).

2. 4. 5. 2. Antioxidative enzymes and non-enzyme antioxidants status

The collected mycelia derived from the respective treatment was homogenised with PBS. The homogenate was centrifuged at 10000 ×g; the supernatant thus obtained was used as the source for antioxidative assays. MDA quantification was done by Aravind and Prasad, (2003). Determination of CAT, SOD, and POD activity was conducted by Zhang et al. (2016b).

Estimation of reduced glutathione was done by standard method. The homogenate derived from respective treatment group (500µL (in 0.1M potassium phosphate buffer (pH7.4)) was precipitated by the inclusion of 4% sulfosalicylic acid (500 µL). The reaction mix was incubated at 4°C for 1 h followed by centrifugation for 20min at 1200 ×g. The supernatant (33µL) thus obtained was mixed with 900µL of 0.1M potassium phosphate buffer (pH7.4) and 66µL of 100mM dithiobis (2-nitrobenzoic acid) (DTNB). GSH reacts with DTNB and produces a yellow coloured complex. The absorbance of the chromogenic products thus obtained was measured at 412 nm.

2.4.5.3. Relative genes expression pattern of first-line antioxidant enzyme biomarkers

Nanocomposite induced oxidative stress was studied by determination of relative gene expression of catalase (CAT), superoxide dismutase (SOD) and peroxidase (POD) genes adopting qRT-PCR. Primers of the respective gene were presented in a table designed with the NCBI Primer-BLAST tool.

2.4.5.3.1. RNA isolation

Biomass derived from the respective treatment was used for RNA extraction. RNA isolation was done using TAKARA RNA iso plus reagent as per the manufacturer's protocol. The isolated RNA was analysed on a 0.8 % agarose gel containing 1 mg/mL ethidium bromide, 6 µL of the PCR products with 4 µL of 6 X gel loading dye were loaded into wells and electrophoresis was performed in 1 X TAE buffer at 50 V for 2 h. The gel was visualised under UV and photographed, and the concentration was calculated as follows

2.4.5.3.2. cDNA synthesis

The first-strand cDNA was synthesised from 20 ng of total RNA by reverse transcription method using Prime Script 1st strand cDNA Synthesis Kit form TAKARA following the manufacturer's instruction.

2.4.5.3.3. qPCR Analysis

qPCR using SYBR green dye (Roche), and analysis of gene expression of oxidative stress enzymes – catalase (CAT), superoxide dismutase (SOD 1), peroxidase (POD) was done by the 2−ΔΔCt method. Per 5µL of the reaction mix, 10 picomolar each of forward and reverse primer, 200 ng cDNA, 1x reaction mix were used. The reaction was carted out in a real-time PCR machine, LightCycler® Nano, Roche. The negative control was used is No template control (NTC). The real-time PCR conditions are according to the manufacture instruction as follows: initial denaturation at 95°C for 10 min, subsequently by 45 cycles of three-step amplification consisting of denaturation at 95°C for 15s, annealing 60°C for 15s and extension at 72°C for the 30s. The melting curve was analysed from 60°C to 95°C for the 20s. At the threshold level, the target gene expression has its own (CT) amplification value.

2.5. Release Profile study

The effect of solvents on the release of natamycin from the synthesised nanocomposite was studied under *in vitro* conditions. 0.1 g of nanocomposite was suspended in 10 mL of respective solvent (distilled water, ethanol, acetone, phosphate-buffered saline) kept under shaking conditions at ambient temperature (30^{o}C). The respective treatment group was centrifuged at 10,000 ×g for 10 min at a defined time. One portion of the supernatant was collected, filter sterilised, followed by spectrophotometric measurement at 303 nm to calculate the release percentage. Another portion was used for antifungal activity against the tested fungal strain by well diffusion assay as described above.

2.6. Biocompatibility assessment using Wistar rat model

Biocompatibility of the prepared nanocomposite was evaluated against the Wistar rat model by recording behavioural, physiological, haematological, biochemical and histopathological parameters.

Signs of mortality or changes in the parameters mentioned above reveal the toxicity of the administrated nanocomposite.

2.6.1. Experimental studies

2.6.2. determination of behavioural changes

Nanocomposite-induced behavioural changes were determined by recording food, water intake, and body weight at defined periods. Morality was also recorded.

2.6.3. determination of biochemical and haematological parameters

The impact of nanocomposite on the major biochemical parameters reveals the liver function profile, lipid profile, and renal function profile was estimated in serum derived from respective treatment groups. A fully automated biochemical analyser (Bio Rod) was used for this analysis. Followed by respective biochemical parameters evaluation, changes in haematological parameters were recorded. Blood samples from the respective treatment group collected on the 28^{th} day of administration of nanocomposite administration, including control, were analysed for various haematological parameters.

2.6.4. determination of histopathological parameters

The nanoformulation's effect on the histopathology of treated animals was studied. Autopsy samples from the respective group of sacrificed animals were fixed in 10% buffered neutral formalin solution followed by embedding in molten paraffin. Fixed tissues were cut using a microtome (5μm thick), and the tissue sections were stained with haematoxylin and eosin. Stained sections were observed microscopically to determine the changes in tissue architecture.

2.7. Coating of nanocomposite

Coating of nanocomposite onto the bread packaging material (butter paper) was conducted by a simple dispersion method. A known volume of carboxyl methylcellulose as the binder (0. 5 %) was mixed with the nanocomposite (final concentration of 100 μg) stirred for 30 min under magnetic stirrer at ambient condition. Check the binder's efficacy with the nanocomposite; the antifungal assay was done as described above. Spore suspension of the fungal strain was uniformly spread on PDA followed by 0.1mL of the suspension thus prepared into the well. Plates were incubated under 28°C. After the incubation period, the plates were evaluated for the zone of inhibition. A zone of inhibition reveals the antifungal activity of the nanocomposite after mixing with the binding agent.

After confirming antifungal activity, the suspension was gently spread onto the sterile butter paper under aseptic condition, followed by drying in the hot air oven at 50°C for 1 h. FTIR and SEM analysis confirmed the coating. A potassium bromide (KBr) pelletised sample was analysed for recording FTIR spectrum (FT-IR8300). In contrast, an SEM micrograph of the processed sample was recorded using carl –Zeiss Supra 55. Dried coated material thus obtained was used for packaging. Bread slices were wrapped with the

dried packaging material and incubated at ambient conditions for 10, 20 and 30 days. Control was maintained by wrapping the bread slices with uncoated butter paper.

2.7.1. effect of packaging on the proximate composition, antioxidative enzymes status and fungal count of packaged bread samples

Proximate composition of bread samples (incubated for 10, 20 and 30 days) wrapped with nanocomposite fabricated packaging material was done by quantitative measurement of total protein, fat, carbohydrate, fibre and moisture (AOAC, 2000).

The antioxidative enzymes status of the bread samples was also studied and incubated at different periods. A known sample volume (1g) was homogenised with 50 mL of 0.1 M phosphate buffer; the suspension thus obtained was stirred at ambient temperature for 1 h. After stirring, the suspension was centrifuged at 10,000 ×g, and the collected supernatant was filter sterilised under aseptic conditions. Collected filtrate thus obtained was used as the source for antioxidative enzymes. DPPH free radical scavenging activity assay, metal chelating ability assay, ferric reducing antioxidant assay, and total antioxidant capacity assay were conducted to determine the antioxidative enzyme status changes described elsewhere.

The serial dilution method determined the packed bread samples' total viable count (TVC). In this method, 1 g of the sample was homogenised in 100 mL of sterile peptone water followed by serial dilution with the same diluent under aseptic conditions. 1 mL of an aliquot from the respective dilution was spread plated on a PDA plate supplemented with antibacterial antibiotics to prevent bacterial growth. The plates after inoculation were incubated at 30°C for 4 days. After the period of incubation, the fungal colonies were counted and recorded.

2.8. Statistical analysis

The experiments were conducted in triplicates, including control. A suitable statistically significant test was analysed to determine the significance of the results.

3. Results And Discussion

Nanotechnology could offer benefits in various fields of food technology. It can bring changes in processing, storage, packaging, food safety, and the development of functional foods for health promotion (Gustavsson et al., 2011). Among the various nanotechnology applications in the food sector, the delivery of antimicrobial agents required to prevent or inhibit microbial growth via nanoencapsulation or other nanotechnology principles has been extensively used in the food industry. Starch colloid filled with the antimicrobial agent operates. When microorganisms grow on the packaged food, they break the starch coating, leading to the release of antimicrobial agents (Kiss, 2020). In this study, gum acacia – gold nanocomposite fabricated with antifungal preservative agent natamycin was prepared via green science principles and the synthesised nanocomposite was evaluated for antifungal activity against

fungal strain *Aspergillus ochraceopealiformis* associated with expired bread sample. Biocompatibility of the nanocomposite was also checked with the Wistar rat model by Determining changes in behavioural, biochemical, haematological and histopathological parameters. The nanocomposite thus studied was coated on the food packaging material, followed by evaluating the proximate composition, antioxidative enzymes and fungal growth of packed bread samples.

3.1. Synthesis of gum acacia gold nanocomposite grafted Natamycin (GA-AuNC-NAT)

A simple in situ green science principle was adopted to synthesise gum acacia gold nanocomposite grafted Natamycin (GA-AuNC-NAT). Initially, gold nanoparticles were synthesised by reducing gold (III) chloride with chitosan as a reducer. Synthesis of AuNps using chitosan as the reducing agent in this study was confirmed by converting the reaction mixture into ruby red (Fig 1a). Furthermore, the determination of surface plasmon resonances by UV visible spectrophotometer also ensures the synthesis. It is known that the surface plasmon resonances (SPR) property of metal nanoparticles is unique with their type of metals, size and shape. After observing the reaction mixture colour change, SPR measurement using a UV visible spectrophotometer is conducted, revealing the absorption band at 530 nm. The formation of AuNps was thus inferred from this SPR measurement (Fig 1b).

Further Characterisation was done by FTIR analysis which was used to record the functional group. For example, FTIR spectra depicted in the Fig 2b shows the strong peaks at 3433 cm^{-1} (belongs to amino and hydroxyl group of chitosan), combined peaks at 2924, 2852 cm^{-1} (C-H stretching vibration of CH_2 symmetry), 1641, 1460 cm^{-1} (C=O stretching of amide bonds). All these findings indicate the role of chitosan as a stabiliser or capping agent responsible for reducing metal precursors into gold nanoparticles.

The selected analytical method characterised the specific interaction of AuNps with the gum acacia-natamycin to transform into a highly stable nanocomposite. A notable change in the colour from deep ruby red into pale pinkish-red (Fig 1a) followed by a shift in the SPR primarily confirms the fabrication of natamycin with gum acacia- gold nanocomposite (Fig 1c). A marked shift of SPR with the retention at 530 nm and SPR at 270-311 nm, which are specific to gum acacia- Natamycin, reveals the specific structural modification.

FTIR analysis was done to determine the possible interaction of polymer natamycin with the gold nanoparticles and structurally modified into nanocomposite (Fig 2). FTIR spectra of free natamycin that presented in Fig 2 a shows 2927.94 cm^{-1} wavenumber lies in between the range of 3000-2850 $cm^{-1,}$ which shows that C-H bond stretch is present and they belong to the functional group of alkanes, 1714.72 cm^{-1} wavenumber lies in between the range of 1725-1700 cm^{-1} which shows that C=O bond stretch is present and they belong to the functional group of ketones, 1643.35 cm^{-1} wavenumber lies in between the range of 1680-1640 cm^{-1} which shows that –C=C- stretch bond is present and they belong to the functional group of alkenes, 1274.95 cm^{-1} wavenumber lies in between the range of 1300-1150 cm^{-1} which shows

that C–H wag $(-CH_2X)$ bond is present, and they belong to the functional group of alkyl halides, 1107.14 cm^{-1} wavenumber lies in between the range of 1250-1020 $cm^{-1,}$ which shows that C-N bond stretch is present. They belong to the functional group of aliphatic amines. Gum acacia FTIR spectra were presented in Fig 2c, indicating functional groups of the polymer. Fig 2d reveals the FTIR spectra of gum acacia. A notable change in the FTIR spectrum was observed after fabrication with AuNps-Natamycin with the gum acacia. Characteristic changes in the absorption peaks due to functional groups' specific interaction between polymer-natamycin and the gold nanostructure.

The structural properties of the synthesised nanocomposite were further evaluated by atomic force microscopy (AFM) and scanning electron microscopy (SEM). AFM is an important technique to analyse the surface topology, revealing dissolution and agglomeration patterns. The AFM micrograph (2D and 3D) depicted in Fig 3a shows the well-distributed nanostructural, spherical homogenous particles without defects or holes. Particle size analysis and distribution were measured with a Zeta sizer at 25 ^{0}C with a 15° scattering angle. The refractive index of the water medium was 1.330. from particle size analysis, the average size of the particles is 325.2 d.nm (Fig 3 b). The SEM analysis with Carl Zeiss Supra 55 reveals the well dispersed, homogenous spherical particles with the size ranging from 80-90 nm (Fig 3 c). SEM micrograph also demonstrates moderate smooth morphology nano dimensional particles with electron scarce thin polymer coating shell. The thermogravimetric analysis was run to determine the thermal stability of the synthesised nanocomposite by Determining weight loss concerning rising temperature. The Thermogravimetric plot in Fig 3d shows that a gradual weight loss of nanocomposite was recorded when the temperature was increased. Therefore, the temperature range was stopped at a high temperature to prevent the inactivation of natamycin from the nanocomposite as it plays a significant part in the therapeutic application.

3.2. Antifungal activity

3.2.1. Fungal strain

The antifungal activity was evaluated against the fungal strain *Aspergillus ochraceopealiformis* isolated from expired bread samples. Among the 10 samples evaluated, the fungal strain was isolated from all the expired samples. Serial dilution culture-dependent method using PDA medium was used for isolation. Most of the fungal colonies recorded in the five expired samples reveal the same morphology. The colony morphology and microscopic examination of spores reveal the isolated strain was *Aspergillus ochraceopealiformis.* PDA plate shows well sporulated yellow colour moderate dense colonies. The microscopic examination reveals the yellow to pale brown conidiophores with globose vesicles. 2.5-3.5 µm size dry, granular conidia were arranged as upright chains. Further Characterisation of the fungal strain was done with 18S rRNA sequencing. The nucleotide sequences of 18S rRNA were subjected to blast analysis with NCBI database, sequences were aligned, and the phylogenetic tree was fabricated using molecular evaluation genomic analysis, revealing 99.0 % similarity with *Aspergillus ochraceopealiformis* (Fig 4).

3.2.2. Antifungal activity

Antifungal activity was studied against the tested fungal strain by determining growth inhibition through well diffusion and liquid assays. Fungal hyphal fragmentation or breakage assay and spore germination inhibition assay was also used to study antifungal efficacy. It has been shown that all the dosages of the nanocomposite resulted in higher antifungal activity. Initially, a well diffusion assay was used to determine antifungal activity, revealing that all the tested concentrations of nanocomposite inhibited the fungal strain. Results were represented as a growth inhibition percentage which shows the tested fungal strain was susceptible to all the dosages of nanocomposite (Fig 5a). The higher growth inhibition rate was recorded in all the dosages of the nanocomposite, demonstrating the uniqueness of the synthesised nanocomposite. Growth inhibition was determined as low at all the dosages of free natamycin. No growth inhibition was observed in gum acacia and the free AuNps. The effect of nanocomposite on fungal growth was further studied by measuring the biomass yield (Fig 5b). Biomass of the fungal strain grown in liquid media with different dosages of free natamycin and free AuNps. gum acacia and the nanocomposite were measured. Results indicate that the fungal growth was inhibited significantly at the nanocomposite with all the concentrations ($P>0.01$ %). Drastic reduction of biomass weight was noticed at the nanocomposite treatment, and no marked effect was observed in free AuNps and gum acacia as in control. Further confirmation of nanocomposite-induced antifungal activity was studied by fungal hyphal fragmentation or breakage assay, representing fragmentation efficacy. Treatment of the fungal strain with the nanocomposite showed a drastic increase in fragmentation efficacy (Fig 6). Free natamycin and AuNps brought about fragmentation in a dose-dependent manner. However, the rate of fragmentation was lower than the nanocomposite. Fig 6b depicts the microscopic examination of fungal strain treated with a high dosage of F-natamycin, AuNps, gum acacia and nanocomposite (100 µg/mL) by a modified method of slide culture technique. Microscopic images reveal that the nanocomposite treatment completely degraded fungal hyphae into more tiny, inert fragments. No structural changes in fungal hyphae, fragmentation, or other structural modification were recorded in gum acacia treatment. Nanocomposite-induced spore germination impact was also studied to determine antifungal activity. Results clearly show the spore germination was inhibited effectively in the nanocomposite treatment (Fig 7 a). Interestingly, high dosages of free natamycin, free gold nanoparticles, gum acacia were also known to cause a marked effect on the spore germination, which was easily inferred from the microscopic examination of fungal spores depicted in Fig 7 b. Spores germinated into a tubular structure as hypha in the control group. In the case of nanocomposite treatment, spore germination was not recorded. The micrograph shown in Fig 7b indicates a spherical, non-tubular structure (non-germinated spores), revealing the spore germination inhibition efficacy. Morphological changes of the fungi in the respective treatment group were analysed by scanning electron microscopy (SEM) SEM micrograph depicted in Fig 7 (i) reveals characteristic changes in the vegetative and reproductive structure of the fungi. Among the various treatment, nanocomposite brought about a notable reduction in the structural dimension. The Control group demonstrates a well-defined conidiophore with smooth-walled globose conidia with distinct dimensions. In nanocomposite treatment, characteristic changes in the regular morphology or dimension were noticed. Organised fungal

morphology was drastically disrupted in the nanocomposite treated fungi. Here, we could not distinguish between vegetative and reproductive structures. The fungal hyphae were agglomerated with a disorganised reproductive structure. This condition was also noticed in free natamycin, free AuNps. However, the degree of morphological changes was lower than the nanocomposite. However, none of the morphological changes was recorded in gum acacia treatment. Nanocomposite induced various oxidative stress markers in the tested fungal strain we reported in this study (described below), the major factor for this morphological change. A transition from the original structure to abnormal morphology reveals the nanocomposite's potential antifungal effect. Previous reports demonstrate the antifungal activity of natamycin against various fungal strains associated with life-threatening fungal infection. Natamycin blocks fungal growth by binding to ergosterol specifically without permeabilising the membrane. Various studies also revealed that natamycin inhibits the growth of yeasts and fungi via the instant inhibition of amino acid and glucose transport transversely to the plasma membrane. In this present study, the nanoformulated natamycin as gum acacia –gold nanocomposite shows a high rate of antifungal activity against the tested fungal strain by recording maximum zone of inhibition, high fungal fragmentation efficacy and spore germination inhibition potential than free natamycin, which all findings indicate the uniqueness of nanocomposite than free natamycin. It can be seen that the unique surface chemistry of gum acacia brought about sustained or controlled release of natamycin that doped with gold nanoparticles. This potential nanocarrier, in turn, triggers enhanced antifungal activity. Gum acacia is an important water-soluble polymer used for nanocomposite readiness. Polymer used in this study, gum acacia, obtained from acacia trees, exhibits distinct physicochemical properties. Carboxyl and amino groups of gum acacia interact with the various functional groups of drugs, improving the adsorption and release kinetics. Gum acacia is also known for its best biocompatibility and biodegradability (Namasivayam et al., 2021). All these properties are used to stabilise metallic nanoparticles doped with specific target molecules having potential biological activities. Liu et al., (2019) have recently studied the antifungal activity of chitosan nanoparticles loaded Natamycin against *Candida albicans* and observed that the Natamycin activity was higher than free natamycin. Natamycin-embedded lecithin-CTS adhesion nanoparticles using CTS crosslinking has been formulated by Bhatta et al., (2012). The enhanced antifungal activity of biopolymers coated natamycin against fungal strains also suggest the possible utilisation of polymers in the delivery of antimicrobial agents in the food sector (Türe et al., 2008). Table 1 reveals the comparison of various nanomaterials based on antifungal activity, and the present findings confirm the noteworthy antifungal activity of tested fungal strain *Aspergillus ochraceopealiformis*. The molecular mechanism of antifungal activity by measuring oxidative stress markers genes studied in this present investigation demonstrates the uniqueness of the nanocomposite.

3.2.3. Oxidative stress induction

Diverse nanomaterials trigger a potential effect on the growth and multiplication of microorganisms via certain oxidative stress-mediated mechanisms. The molecular mechanism of antifungal activity induction by oxidative stress has gained more attention in developing antifungal agents. Studying antioxidative responses like antioxidants (antioxidative enzymes and non-enzyme antioxidants) towards the oxidative stress induced by nanomaterials is an important criterion for utilising

nanotechnology principles to fight against fungal organisms (Krishnan et al., 2017). In this present study, the level of ROS generation, antioxidative enzymes like CAT, SOD, POD, and non-enzyme antioxidant GSH in the tested fungal strain exposed to different nanocomposite dosages were investigated. To check the efficacy, we evaluated free NT, AuNps and GA-AuNC. Oxidative stress in response to nanocomposite exposure was assessed by measuring reactive oxygen species. The oxidative stress in a feedback mechanism is triggered by Reactive Oxygen Species (ROS), which leads to many biological processes, such as Necrosis, Apoptosis and Autophagy. The overwhelming production of ROS can destroy organelle's structure and bio-molecules (Delattin et al., 2014). It was observed that nanocomposite exposure increased ROS generation significantly (P>0.01 %). There was no significant difference recorded between free natamycin and free AuNps. Free gum acacia resulted in no marked ROS generation compared with other treatments (Fig 8). The quantity of ROS produced by metallic NPs correlates with particle size, shape, surface area, and chemistry. ROS possess several functions in cellular biology, with ROS generation a vital factor in metallic NP-induced toxicity, as well as modulation of cellular signalling involved in cell death, proliferation, and differentiation (Ighodaro et al., 2018). Elevated ROS generation observed in the present study clearly shows that the nanocomposite, due to its unique physicochemical properties, may trigger oxidative stress in the fungal strain, resulting in more ROS and fungal death. Oxidative stress in the tested fungal strain exposed to nanocomposite was also studied by measuring MDA content (Fig 9). It was observed that nanocomposite treatment caused a significant increase in MDA content (P>0.01 %). This finding indicates that the oxidation of lipids is mediated by free radicals induced by nanocomposite treatment. Free natamycin, AuNps exposure also recorded an increase in MDA content. However, the level was found to be lower than the nanocomposite. No marked difference was found between the control and gum acacia treatment groups.

Oxidative stress markers induction by the nanocomposite was further studied by quantifying enzymatic and non-enzymatic antioxidants, including CAT, SOD, POD, and GSH, respectively. Antioxidant enzymes are a strong defence against ROS-induced damage; modulation in these enzyme activities responded to increased ROS generation induced by the nanocomposite treatment (Deponte, 2013). In this study, increases in these enzyme activities respond to increased ROS generation. It is well known that fungi are an important group of organisms showing a marked response to oxidative stress in producing various antioxidants. The determination of antioxidants reveals the oxidative status of the fungal strains, affecting the survival or growth parameters.

Quantitative measurement of three major oxidative stress marker genes like CAT, SOD and POD expression by qRT-PCR was conducted to determine the nanocomposite induced effect on the molecular mechanism of antifungal activity. Total RNA was isolated from the respective treatment group, followed by cDNA synthesis. Synthesised cDNA amplified with the primers of the respective genes, and the data were analysed by the comparative c1 method. The expression of the cDNA pattern in the respective treatment shown in Fig 9 indicates the marked effect of the nanocomposite. Unlike sharp, thick or dense cDNA bands that appeared in the control group, less dense or thin cDNA bands were observed in nanocomposite treatment. No changes in the cDNA expression pattern were recorded in gum acacia treatment as in control groups. Relative gene expression study reveals the nanocomposite with all the

tested concentrations brought about a drastic reduction of relative gene expression of respective genes (Fig 10). An increase in expression reduction was recorded in free natamycin and free AuNps, whereas no reduction in the gene expression was observed in gum acacia treatment. The drastic reduction or notable modulation of the marker genes is due to potent oxidative stress triggered by the nanocomposite, which affects the activity and total content of enzymatic antioxidants and non-enzymatic antioxidants.

The effect of nanocomposite on the enzymatic and non-enzymatic antioxidants was investigated. CAT is a common antioxidant enzyme that catalyses the degradation of hydrogen peroxide into water and molecular oxygen. The highly efficient CAT can break down millions of H_2O_2 molecules. The facility of CAT to effectively limit H_2O_2 concentration in cells emphasises its importance in the aforementioned physiological procedures and is the first line antioxidant defence enzyme (Aggarwal and Shishodia, 2006). Superoxide dismutase (SOD) is the most potent endogenous antioxidant enzyme that acts as a first-line defence system against reactive oxygen species (ROS). The two molecules of superoxide anion (O_2) to hydrogen peroxide (H_2O_2) and molecular oxygen (O_2) were catalysed by the dismutation process. Since it is an important enzymatic antioxidant defence against various physiological stresses related conditions, the level of SOD activity determines the health status of the cells (Casagrande et al., 2014). Nanocomposite treatment significantly enhanced CAT, SOD and POD activity ($P>0.01$ %). A concentration-dependent increase in the enzyme activity was noticed in free natamycin and free AuNps treatment. No impact on all the tested enzymatic antioxidants was recorded in gum acacia treatment as in the control group (Fig 11). The response of non-enzymatic antioxidant GSH was also measured in the respective treatment group (Fig 11 e). GSH is a non-enzymatic antioxidant that protects the cells from oxidative stress and thus maintains the cellular redox status (Huang et al., 2017). Nanocomposite treated fungal strain accumulated more GSH than the remaining treatment groups. Maximum GSH content was observed in all the dosages of nanocomposite treatment. Dose-dependent variation in GSH content was recorded in free natamycin and free AuNps treatment, whereas no marked effect was recorded in gum acacia treatment.

3.3. Release profile studies

Effect of solvents like distilled water, phosphate-buffered saline, acetone and ethanol on the release of natamycin was studied by spectrophotometric Determination of Natamycin released in the respective solvents. Results were represented by release percentage concerning the different time intervals. All the solvents reveal a sustained or controlled pattern of Natamycin (Fig 12). In general, all the solvents show initial burst release at 72 h followed by a gradual increase concerning the period. The maximum cumulative release of 90.0 %, 94.1 %, 90.0 %, and 98.2 % was recorded at 144 h in distilled water, PBS, acetone, and ethanol. It can be seen that the initial burst release is an essential criterion of antifungal activity as it helps reach the therapeutic concentration of the drug in a minimal period, followed by constant release to maintain the sustained and controlled release of the drug (Jiang et al., 2020). Antifungal activity of natamycin released in the respective solvents at the respective period was evaluated against the fungal strain by well diffusion assay as described earlier. The zone of inhibition depicted in Fig 12 e - h reveals that the released natamycin in all the solvents retained the antifungal

activity. Unique surface chemistry of gum acacia brought about sustained or controlled release of natamycin that doped with gold nanoparticles – a potential nanocarrier that triggers enhanced antifungal activity.

3.4. Biocompatibility

Biocompatibility of the synthesised nanocomposite was studied by acute, sub-acute toxicity studies with the Wistar rat model. Determination of changes in routine behaviour (Food, Water intake, sign of mortality), changes in organ weights, biochemical (Liver & Renal function), haematological and histopathological parameters of an animal model that administrated with low (300 mg/Kg) and high (600 mg/Kg) dosages of the nanocomposite. Mortality was also checked in the respective treatment group. Results indicate the nanocomposite treatment was not inducing any sign of undesirable changes in behaviour, biochemical, haematological and histopathological parameters. Mortality was also not recorded in both the dosages, indicating that the tested nanocomposite seems safe. Reports suggest that any bioactive agent used as a pharmacological application in the single oral dose of 250 and 500 mg/Kg is nontoxic (Saleh et al., 2016).

Initial studies on the effect of nanocomposite on the bodyweight of nanocomposite administered animal group were studied. Results depicted in Fig 13 shows no undesirable effect on the bodyweight of tested animals of both sexes at all the tested periods. Significant changes were not recorded in tested animals' food and water intake and body weight. Reports reveal that decreased or increased body or organ weight is due to drug-mediated physiological stress. The food and water intake quantity were the same as the control group (Fig 13 b, c). Nanocomposite induced effect on the weight of vital organs was also investigated. The absence of marked undesirable differences in the weight of vital organs, as shown in Fig 14, reveals the outstanding biocompatibility. No mortality was observed during the whole period of bioassay studies. No abnormal deviations were observed. No substantial changes were observed in the values of different parameters studied compared with controls and values obtained within normal laboratory limits.

The impact of nanocomposite on the biochemical, haematological and histopathological parameters was investigated. In the biochemical parameters evaluated, nanocomposite treatment groups recorded no significant changes (Fig 15). As in control, nanocomposite treatment groups have also exhibited values within laboratory limits. It has been suggested that notable changes in the biochemical parameters are due to the undesirable effect of compounds or drugs on the various vital organs like the liver. Various adverse effects like acute inflammation, cellular leakage, and liver cell membrane damage due to the interaction of the drugs with the liver elicit notable changes in the various biochemical parameters. In this study, no marked impact on the biochemical parameters of the treatment groups confirms the best biocompatibility. As in diverse biochemical parameters evaluated, nanocomposite induced impact on the haematological parameters like haemoglobin (Hb), red blood cell (RBC), white blood cell (WBC), packed cell volume (PCV) was studied using an autoanalyser. Results represented in Fig 15 indicate that both the nanocomposite's dosages were not shown any marked impact.

Biocompatibility was also confirmed by histopathological examination of tissue sections derived from respective treatment groups adopting standard methods. Histopathological results clearly show the nanocomposite was not inducing any significant changes, abnormalities or tissue alteration (Fig 16). This study investigated histopathological examination of heart, lungs, liver and kidneys tissue derived from the respective treatment group. In the case of heart tissue, nanocomposite treatment did not induce any undesirable myocardial tissue changes. Myocardial tissue derived from the nanocomposite treatment group showed no sign of inflammation. Myocardial tissue shows no oedema or stroma without lymphocytic infiltration, indicating no myocyte degeneration or inflammations. Liver histopathology also indicates no sign of the undesirable effect. Notable or marked changes in hepatocytes were not recorded in the nanocomposite treatment group as in control. There was no lymphocyte infiltration, central vein congestion, sinusoid dilations, and bile duct hyperplasia in nanocomposite treatment groups. Histopathological analysis of the spleen also demonstrates the best biocompatibility. No structural modification or abnormalities in a marked sign of inflammation with high lymphocyte infiltration were recorded in nanocomposite treatment groups. Kidney tissue histopathological analysis also confirms the best biocompatibility. Cortex and medulla were not exhibited any structural modification or alteration. No marked changes in the glomeruli structure were observed in nanocomposite treatment groups. No evidence of infiltration in the interstitium and blood vessels congestion conforms to the renal safety or biocompatibility of the nanocomposite.

3.5. Nanocomposite coating on the bread packaged material

The antifungal activity of the nanocomposite with carboxyl methylcellulose that was used for coating on packaging material was done to evaluate the effectiveness of nanocomposite. Antifungal activity of the nanocomposite mixed with CMC was conducted before coating. The well diffusion assay reveals the tested fungal strain was susceptible to the nanocomposite with CMC by recording a well-defined zone of inhibition with 17.0 mm (Fig 17a). This finding indicates that the addition of CMC was not affecting the effectiveness of the nanocomposite and the nanocomposite still retained the antifungal property. A simple dispersion method was adopted to coat nanocomposite onto bread packaged material-butter paper selected in this study (Fig 17). This finding indicates that the nanocomposite retained the antifungal activity after mixing with CMC.

Further confirmation of coating was done by scanning electron microscopy analysis of packaged material. SEM micrograph shown in Fig 17 b, c indicates the nano dimensional particles were uniformly coated on the surface of the packaged material. It can be seen that the size shape of the nanocomposite that coated on the packaging material was also not changed. The well-dispersed nanocomposite was embedded into the fibre surface. A previous study suggests that particles size play a significant role in fabrication (Namasivayam et al., 2021). Larger agglomerate particles may be removed from the fibre surface while smaller nano dimensional particles penetrate deeply and adhere strongly. The nano dimensional structure of the composite material proposed in this study confirms the adherence of the particles deeply into the fibre surface.

3.6. Effect of coating on the proximate composition, antioxidative enzymes and fungal growth

Bread slices packed with nanocomposite fabricated packaging material were checked for changes in proximate composition, antioxidative enzymes and fungal growth. Bread has always been one of the extremely prevalent and appealing foodstuffs due to its top-quality nutritional, sensorial and textural characteristics, ready to eat convenience, and cost competitiveness. Bread is highly susceptible to pathogenic microorganisms due to its high nutrient content. Spoilage may occur during storage. Packaging with antimicrobial agents coated materials protect the bread or other items from pathogenic invasion or spoilage. In this study, the biocompatible nanocomposite was coated on butter paper. Bread slices were covered with this packaging material. The effect of nanocomposite coated package on the quantitative measurement of total protein, fat, carbohydrate, fibre and moisture content was done by the modified method of AOAC (Brothers and Wyatt, 2000). It shows a significant difference in proximate composition between treatment groups concerning the incubation period (Fig 18 a). The Control group revealed a sharp decrease in all the tested parameters at the respective incubation period. The control group drastically reduced all the tested proximate compositions as the storage time increased. Unlike the control group, the nanocomposite treatment group showed no marked difference in proximate composition. This finding indicates that the nanocomposite packaging was not inducing any undesirable effect. The antioxidative enzymes status of the packaged bread samples was also checked. It is well known that the level of antioxidative enzymes is primarily determined by oxidative stress. Oxidative stress is a convoluted chemical and physiological spectacle that arises due to excessive production and accumulation of reactive oxygen species, which cause severe damage to the cells (Krishnan et al., 2017). Antioxidative enzymes like catalase, superoxide dismutase and glutathione reductase are the major enzyme-based components in detoxifying the reactive oxygen species (Namasivayam et al., 2021). Measurement of antioxidative enzymes plays a vital role in determining oxidative stress. Among the treatment groups, no changes in all the tested antioxidative enzymes activity were recorded in nanocomposite packaged bread samples (Fig 18 b). All the tested antioxidative enzyme activity was high in control, revealing that the bread samples were susceptible to fungal growth and oxidative stress induction. In response to this stress, antioxidative enzymes may produce effectively. In the case of nanocomposite packaged bread slices, no fungal growth was observed, which in turn causes no oxidative stress. Fungal growth was determined by the serial dilution method, which indicates that more fungal colonies were observed in the control group at all the tested periods (Table 2). No fungal growth was recorded in the nanocomposite treatment group. Membrane chemistry of gum acacia facilitates the sustained or controlled release of gold nanoparticles- natamycin nano-drug conjugate, which is used to fight against fungal cells.

4. Conclusion

In this present investigation, antifungal food preservative agent natamycin was formulated as gum acacia-gold nanocomposite by simple in situ green science principles. Synthesised nanocomposite exhibited high structural, functional stability with the notable antifungal activity against fungal strain isolated from expired bread sample *Aspergillus ochraceopealiformis*. The molecular mechanism of

antifungal activity was studied by measuring oxidative stress markers, which reveals a notable elevation of oxidative stress induced by nanocomposite. Release profile studies with different solvents also reveal the marked controlled or sustained release pattern. Furthermore, he synthesised nanocomposite's acute and sub-acute toxicity was evaluated with the Wistar animal model, demonstrating a high rate of biosafety or biocompatibility. Fabrication of the nanocomposite on butter paper used as packaging material for bread slices. Followed by packaging, the level of antioxidative enzymes the proximate composition was determined. Nanocomposite packaging was not shown any undesirable effect on antioxidative enzymes and proximate composition. Fungal growth was not recorded in nanocomposite packaging. Further study will be helpful to use the nanocomposite thus synthesised as an effective, safe food preservative agent against a wide range of food spoilage organisms.

Declarations

Acknowledgement

We acknowledge SIST for the Characterisation of the nanocomposite. Special thanks to Dr Hari Hara Sivakumar, Professor, Department of Pharmacology, KMCH College of Pharmacy, Coimbatore, Tamil Nadu, for assisting in biocompatibility animal model studies.

Compliance with Ethical Standards:

This research did not receive any explicit grant from funding agencies in the public, commercial, or non-profit sector.

Conflicts of interest

We declare no conflicts of interest.

References

1. Chaudhry, Q., Scotter, M., Blackburn, J., Ross, B., Boxall, A., Castle, L., Aitken, R., & Watkins, R. (2008). Applications and implications of nanotechnologies for the food sector. In Food Additives and Contaminants - Part A Chemistry, Analysis, Control, Exposure and Risk Assessment (Vol. 25, Issue 3, pp. 241–258). https://doi.org/10.1080/02652030701744538

2. Wu, H., Liu, W., Shi, L. *et al.* Comparative Genomic and Regulatory Analyses of Natamycin Production of *Streptomyces lydicus* A02. *Sci Rep* **7,** 9114 (2017). https://doi.org/10.1038/s41598-017-09532-3

3. Parada, J. L., Caron, C. R., Medeiros, A. B. P., & Soccol, C. R. (2007). Bacteriocins from lactic acid bacteria: Purification, properties and use as biopreservatives. Brazilian Archives of Biology and Technology, 50(3), 521–542. https://doi.org/10.1590/s1516-89132007000300018

4. S. Karthick Raja Namasivayam S. Samydurai, Vinay Kumar Pandey. 2016. Influence of Algal Based Protein Nanoparticles Loading on Antibacterial Activity, *In Vitro* Drug Release and Cytotoxicity of Cephalosporin Derivative. *Asian Journal of Pharmaceutics* 10 (4); 595-599

5. Namasivayam, S. K. R., Angel, J. C. R., Bharani, R. S. A., & Karthik, M. Y. (2014). Effect of media on bacteriocin production by Lactobacillus brevis and evaluation of antibacterial activity. Research Journal of Pharmaceutical, Biological and Chemical Sciences, 5(5), 1129–1136.

6. Du, Y. L. *et al*. Identification of a novel *Streptomyces chattanoogensis* L10 and enhancing its natamycin production by overexpressing positive regulation scnRII. *J. Microbiol.* **47**, 506–513 (2009).

7. Pedersen J.1992. Natamycin as a fungicide in agar media. Applied and Environmental Microbiology,58; 1064-1066

8. Leyva Salas, Marcia et al. “Antifungal Microbial Agents for Food Biopreservation-A Review.” *Microorganisms* vol. 5,3 37. 8 Jul. 2017, doi:10.3390/microorganisms5030037

9. de Boer, E. & Stolk-Horsthuis, M. (1977) Sensitivity to natamycin (pimaricin) of fungi isolated in cheese warehouses. *J. Food Prot.*, **40**, 533–536.

10. Aparicio, J.F., Colina, A.J., Ceballos, E. & Martin, J.F. (1999) The biosynthetic gene cluster for the 26-membered ring polyene macrolide pimaricin. *J. Biochem. Mol. Biol.*, **274**, 10133–10139.

11. Te Welscher, Y. M., Ten Napel, H. H., Balagué, M. M., Souza, C. M., Riezman, H., De Kruijff, B., & Breukink, E. (2008). Natamycin blocks fungal growth by binding specifically to ergosterol without permeabilising the membrane. Journal of Biological Chemistry, 283(10), 6393–6401. https://doi.org/10.1074/jbc.M707821200

12. Delattin, N., Cammue, B. P., & Thevissen, K. (2014). Reactive oxygen species-inducing antifungal agents and their activity against fungal biofilms. Future Medicinal Chemistry, 6(1), 77–90. https://doi.org/10.4155/fmc.13.189

13, Te Welscher, Y. M., Van Leeuwen, M. R., De Kruijff, B., Dijksterhuis, J., & Breukink, E. (2012). Polyene antibiotic that inhibits membrane transport proteins. Proceedings of the National Academy of Sciences of the United States of America, 109(28), 11156–11159. https://doi.org/10.1073/pnas.1203375109

14. Lalitha, P., Shapiro, B. L., Srinivasan, M., Prajna, N. V., Acharya, N. R., Fothergill, A. W., Ruiz, J., Chidambaram, J. D., Maxey, K. J., Hong, K. C., McLeod, S. D., & Lietman, T. M. (2007). Antimicrobial susceptibility of Fusarium, Aspergillus, and other filamentous fungi isolated from keratitis. Archives of Ophthalmology, 125(6), 789–793. https://doi.org/10.1001/archopht.125.6.789

15. Lalitha, P., Vijaykumar, R., Prajna, N. V., & Fothergill, A. W. (2008). In vitro natamycin susceptibility of ocular isolates of Fusarium and Aspergillus species: Comparison of commercially formulated natamycin

eye drops to pharmaceutical-grade powder. Journal of Clinical Microbiology, 46(10), 3477–3478. https://doi.org/10.1128/JCM.00610-08

16. Xu, Y., Pang, G., Gao, C., Zhao, D., Zhou, L., Sun, S., & Wang, B. (2009). In vitro comparison of the efficacies of natamycin and silver nitrate against ocular fungi. Antimicrobial Agents and Chemotherapy, 53(4), 1636–1638. https://doi.org/10.1128/AAC.00697-08

17. Brothers AM, Wyatt RD. The antifungal activity of natamycin toward molds isolated from commercially manufactured poultry feed. Avian Dis. 2000 Jul-Sep;44(3):490-7. PMID: 1100699

18. Al-Hatmi, A. M. S., Meletiadis, J., Curfs-Breuker, I., Bonifaz, A., Meis, J. F., & De Hoog, G. S. (2016). In vitro combinations of natamycin with voriconazole, itraconazole and micafungin against clinical Fusarium strains causing keratitis. Journal of Antimicrobial Chemotherapy, 71(4), 953–955. https://doi.org/10.1093/jac/dkv421

19. Rees, C. A., Bao, R., Zegans, M. E., & Cramer, R. A. (2019). Natamycin and voriconazole exhibit synergistic interactions with non-antifungal ophthalmic agents against Fusarium species ocular isolates. Antimicrobial Agents and Chemotherapy, 63(7), e02505-18. https://doi.org/10.1128/AAC.02505-18

20. Abhishakth Gerhardt, B.S., Bhuvaneshwari., Sravani Marpaka. (2019). Effect of topical 5% Natamycin in treatment of fungal corneal ulcer: A prospective study in a tertiary care teaching hospital in Telangana. MedPulse International Journal of Pharmacology, 12(1), 1-5.

21/ Jiang, T., Tang, J., Wu, Z., Sun, Y., Tan, J., & Yang, L. (2020). The combined utilisation of Chlorhexidine and Voriconazole or Natamycin to combat Fusarium infections. BMC Microbiology, 20(1), 1–6. https://doi.org/10.1186/s12866-020-01960-y

22. Liu, J., Wang, J., Song, H., Zhang, Z., Xu, X., Ji, X., & Shi, X. (2019). Antifungal Activity and Mechanisms of Natamycin Against Colletotrichum gloeosporioides in Postharvest Mango Fruit. Chinese Bulletin of Botany, 54(4), 455.

23. Prakash, J., Vignesh, K., Anusuya, T., Kalaivani, T., Ramachandran, C., Sudha, R. R., ... & DevanandVenkatasubbu, G. (2019). Application of Nanoparticles in Food Preservation and Food Processing. Journal of Food Hygiene and Safety, 34(4), 317–324. https://doi.org/10.13103/jfhs.2019.34.4.317

24. Fernandes, A. R., Mendonça-Martins, I., Santos, M. F. A., Raposo, L. R., Mendes, R., Marques, J., Romão, C. C., Romão, M. J., Santos-Silva, T., & Baptista, P. V. (2020). Improving the Anti-inflammatory Response via Gold Nanoparticle Vectorization of CO-Releasing Molecules. ACS Biomaterials Science and Engineering, 6(2), 1090–1101. https://doi.org/10.1021/acsbiomaterials.9b01936

25. Karthick Raja Namasivayam, S., Arvind Bharani, R. S., & Karunamoorthy, K. (2018). Insecticidal fungal metabolites fabricated chitosan nanocomposite (IM-CNC) preparation for the enhanced larvicidal activity

- An effective strategy for green pesticide against economic important insect pests. International Journal of Biological Macromolecules, 120, 921–944. https://doi.org/10.1016/j.ijbiomac.2018.08.130

26. Shahbazi, Y., & Shavisi, N. (2019). Current advancements in applications of chitosan based nano-metal oxides as food preservative materials. Nanomedicine Research Journal, 4(3), 122–129. https://doi.org/10.22034/NMRJ.2019.03.001

27. Mohammadi, A., Hashemi, M., & Hosseini, S. M. (2015). Nanoencapsulation of Zataria multiflora essential oil preparation and Characterisation with enhanced antifungal activity for controlling Botrytis cinerea, the causal agent of gray mould disease. Innovative Food Science and Emerging Technologies, 28, 73–80. https://doi.org/10.1016/j.ifset.2014.12.011

28. Badawy, M. E. I., Lotfy, T. M. R., & Shawir, S. M. S. (2019). Preparation and antibacterial activity of chitosan-silver nanoparticles for application in preservation of minced meat. Bulletin of the National Research Centre, 43(1), 1–14. https://doi.org/10.1186/s42269-019-0124-8

29. Kiss. (2020). Nanotechnology in food systems: A review. Acta Alimentaria, 49(4), 460–474. https://doi.org/10.1556/066.2020.49.4.12

30. Akhavan, S., Assadpour, E., Katouzian, I., & Jafari, S. M. (2018). Lipid nano scale cargos for the protection and delivery of food bioactive ingredients and nutraceuticals. Trends in Food Science and Technology, 74, 132–146. https://doi.org/10.1016/j.tifs.2018.02.001

31. Butnaru, E., Cheaburu, C. N., Yilmaz, O., Pricope, G. M., & Vasile, C. (2016). Poly (vinyl alcohol)/chitosan/montmorillonite nanocomposites for food packaging applications: Influence of montmorillonite content. High Performance Polymers, 28(10), 1124–1138. https://doi.org/10.1177/0954008315617231

32. Leyva Salas, M., Mounier, J., Valence, F., Coton, M., Thierry, A., & Coton, E. (2017). Antifungal Microbial Agents for Food Biopreservation—A Review. Microorganisms, 5(3), 37. https://doi.org/10.3390/microorganisms5030037

33. Sagun-bella, K. Q. De, Agahan, A. L. D., Cubillan, L. D. P., Carino, N. S., & Mesa-rodriguez, R. De. (2013). Antifungal Activity of Voriconazole on Local Isolates: an In-vitro Study. Philipp J Ophthalmol, 38 (June 2013), 29–34.

34. Fahimi, S., & Ghorbani, H. R. (2019). The preparation of chitosan-Ag nanocomposite for food packaging. J. Nanoanalysis, 6(2), 115–120. http://creativecommons.org/licenses/by/4.0/.

35. M Ahmed, E., Saber, D., Abd Elaziz, K., Alghtani, A. H., Felemban, B. F., Ali, H. T., & Megahed, M. (2021). Chitosan-based nanocomposites: Preparation and Characterisation for food packing industry. Materials Research Express, 8(2), 25017. https://doi.org/10.1088/2053-1591/abe791

36. Hooda, R., Batra, B., Kalra, V., Rana, J. S., & Sharma, M. (2018). Chitosan-Based Nanocomposites In Food Packaging. In Bio-based Materials for Food Packaging: Green and Sustainable Advanced Packaging Materials (pp. 269–285). Springer. https://doi.org/10.1007/978-981-13-1909-9_12

37. Masheane, M., Nthunya, L., Malinga, S., Nxumalo, E., Barnard, T., & Mhlanga, S. (2016). Antimicrobial properties of chitosan-alumina/f-MWCNT nanocomposites. Journal of Nanotechnology, 2016, 8.

38. Meghani, N., Dave, S., Kumar, A. (2019). Nanofood and its application–A review. BAOJ Nanotech., 5(1), 1–16.

39. Shanmuga Priya, D., Suriyaprabha, R., Yuvakkumar, R., & Rajendran, V. (2014). Chitosan-incorporated different nanocomposite HPMC films for food preservation. Journal of Nanoparticle Research, 16(2), 1–16. https://doi.org/10.1007/s11051-014-2248-y

40. Kumar, S., Ye, F., Dobretsov, S., & Dutta, J. (2019). Chitosan nanocomposite coatings for food, paints, and water treatment applications. Applied Sciences (Switzerland), 9(12), 2409. https://doi.org/10.3390/app9122409

41. Padmanabhan, V. P., Kulandaivelu, R., & Nellaiappan, S. N. T. S. (2018). New core-shell hydroxyapatite/um-Acacia nanocomposites for drug delivery and tissue engineering applications. Materials Science and Engineering C, 92, 685–693. https://doi.org/10.1016/j.msec.2018.07.018

42. Bhatta, R. S., Chandasana, H., Chhonker, Y. S., Rathi, C., Kumar, D., Mitra, K., & Shukla, P. K. (2012). Mucoadhesive nanoparticles for prolonged ocular delivery of natamycin: In vitro and pharmacokinetics studies. International Journal of Pharmaceutics, 432(1–2), 105–112. https://doi.org/10.1016/j.ijpharm.2012.04.060

43. Boskovic, M., Glisic, M., Djordjevic, J., Vranesevic, J., Djordjevic, V., & Baltic, M. Z. (2019). Preservation of meat and meat products using nanoencapsulated thyme and oregano essential oils. IOP Conference Series: Earth and Environmental Science, 333(1), 12038. https://doi.org/10.1088/1755-1315/333/1/012038

44. Ding, S. J., & Zhu, J. (2015). Tuning the surface enhanced Raman scattering activity of gold nanocubes by silver coating. Applied Surface Science, 357, 487–492. https://doi.org/10.1016/j.apsusc.2015.09.077

45. Coman, C., Leopold, L. F., Rugina, O. D., Diaconeasa, Z. O. R. I. Ţ. A., Bolfa, P. F., Leopold, N. & Socaciu, C. A. R. M. E. N. (2015). Protein-capped gold nanoparticles obtained by a green synthesis method. *Studia UBB Chemia*, *60*, 119.

46. Narendrakumar, G., Karthick Raja Namasivayam, S., Manikanta, M., Saha, M., Dasgupta, T., Divyasri, N., Anusha, C., Arunkumar, B., & Preethi, T. V. (2018). Enhancement of biocontrol potential of biocompatible bovine serum albumin (BSA) based protein nanoparticles loaded bacterial chitinase

against major plant pathogenic fungi *Alternaria alternata*. Biocatalysis and Agricultural Biotechnology, 15, 219–228. https://doi.org/10.1016/j.bcab.2018.05.015

47. AOAC (2000) Official Methods of Analysis. 17th Edition, The Association of Official Analytical Chemists, Gaithersburg, MD, USA. Methods 925.

48. Gustavsson, J., Cederberg, C., Sonesson, U., van Otterdijk, R., & Meybeck, A. (2011). Global food losses and food waste: extent, causes and prevention. International Congress: Save Food! 38. http://www.fao.org/fileadmin/user_upload/ags/publications/GFL_web.pdf

49. Karthick Raja Namasivayam, S., Arul Maximus Rabel., Prasana, R., Arvind Bharani, R. S., Valli Nachiyar, C. (2021). Gum acacia PEG iron oxide nanocomposite (GA-PEG-IONC) induced pharmacotherapeutic activity on the Las R gene expression of Pseudomonas aeruginosa and HOXB13 expression of prostate cancer (Pc 3) cell line. A green therapeutic approach of molecular mechanism inhibition. International Journal of Biological Macromolecules, 190, 940-959.

50. Türe, H., Eroglu, E., Soyer, F., & Özen, B. (2008). Antifungal activity of biopolymers containing natamycin and rosemary extract against *Aspergillus niger* and *Penicillium roquefortii.* International Journal of Food Science and Technology, 43(11), 2026–2032.

51. Krishnan, G. S., Rajagopal, V., Antony Joseph, S. R., Sebastian, D., Savarimuthu, I., Karthick Raja Namasivayam, S., & Thobias, A. F. (2017). *In vitro, in silico and in vivo* antitumor activity of crude methanolic extract of *tetilla dactyloidea (*carter, 1869) on den induced hcc in a rat model. Biomedicine and Pharmacotherapy, 95, 795–807. https://doi.org/10.1016/j.biopha.2017.08.054

52. Delattin, N., Cammue, B. P., & Thevissen, K. (2014). Reactive oxygen species-inducing antifungal agents and their activity against fungal biofilms. Future Medicinal Chemistry, 6(1), 77–90. https://doi.org/10.4155/fmc.13.189

53. Ighodaro, O. M., & Akinloye, O. A. (2018). First line defence antioxidants superoxide dismutase (SOD), catalase (CAT) and glutathione peroxidase (GPX): Their fundamental role in the entire antioxidant defence grid. Alexandria Journal of Medicine, 54(4), 287-293. DOI: 10.1016/j.ajme.2017.09.001

54. Deponte, M. (2013). Glutathione catalysis and the reaction mechanisms of glutathione-dependent enzymes. Biochimica et Biophysica Acta, 1830(5), 3217-66. DOI: 10.1016/j.bbagen.2012.09.018

55. Aggarwal, B. B., & Shishodia, S. (2006). Molecular targets of dietary agents for prevention and therapy of cancer. Biochemical Pharmacology, 71(10), 1397-1421. DOI: 10.1016/j.bcp.2006.02.009

56. Casagrande, J. C., Macorini, L. F. B., Antunes, K. A., Santos, U. P. D., Campos, J. F., Dias-Júnior, N. M., & de Picoli Souza, K . (2014). Antioxidant and cytotoxic activity of hydroethanolic extract from *Jacaranda decurrens* leaves. PLoS ONE, *9*(11), e112748. DOI: 10.1371/journ al.pone.0112748

57. Huang, C., Lai, C., Xu, P., Zeng, G., Huang, D., Zhang, J., Zhang, C., Cheng, M., Wan, J., & Wang, R. (2017). Lead-induced oxidative stress and antioxidant response provide insight into the tolerance of Phanerochaete chrysosporium to lead exposure. Chemosphere, 187, 70-77. DOI: 10.1016/j.chemosphere.2017.08.104.

58. Saleh, H. H., Ali, Z. I., & Afify, T. A. (2016) Synthesis of Ag/PANI core shell nanocomposites using ionising radiation. Advanced Polymer Technology, 35(3), 335–344. DOI:10.1002/adv.21560.

59. Karthick Raja Namasivayam, S., Venkatachalam, G., & Bharani, R. S. A. (2021). Noteworthy enhancement of wound-healing activity of Triphala biomass metabolite-loaded hydroxyapatite nanocomposite. Applied Nanoscience, 11(5), 1511–1530. DOI: 10.1007/s13204-021-01813-8.

60. Villamizar-Gallardo, R., Cruz, J. F. O., & Ortíz-Rodriguez O. O. (2016). Fungicidal effect of silver nanoparticles on toxigenic fungi in cocoa, Pesquisa Agropecuária Brasileira. 51(12), 1929-1936, DOI: 10.1590/S0100-204X2016001200003

61. Akpinar, I., Unal, M., & Sar, T. (2021). Potential antifungal effects of silver nanoparticles (AgNPs) of different sizes against phytopathogenic *Fusarium oxysporum* f. sp. *radicis-lycopersici* (FORL) strains. SN Applied Sciences, 3(4), 506. DOI: 10.1007/s42452-021-04524-5

62. Zhang, F., Liu, X., Pentok, M., Sauli, E., He, N., Zen, X., Li, X., & Li, T. (2019). Molecular mechanism and changes of antioxidant enzyme in ZnO nanoparticles against fungus. Journal of Biomedical Nanotechnology, 15(4), 647-661. DOI: 10.1166/jbn.2019.2718.

63. Basu, A., Ray, S., Chowdhury, S., Sarkar, A., Mandal, D. P., Bhattacharjee, S., & Kundu, S. (2018). Evaluating the antimicrobial, apoptotic, and cancer cell gene delivery properties of protein-capped gold nanoparticles synthesised from the edible mycorrhizal fungus *Tricholoma crissum*. Nanoscale Research Letters, 13, 154. DOI: 10.1186/s11671-018-2561-y

64. Rahimzadeh Torabi, L., & Doudi. M. (2016). The effect of gold nanoparticles compared to dioxide titanium nanoparticles on vital factors of isolated *Candida albicans* in patients with oral candidiasis *in vitro*. Zahedan Journal of Research in Medical Sciences. 18(12), e5666.
DOI : 10.17795/zjrms-5666

65. Folorunso, A., Akintelu, S., Oyebamiji, A. K., Ajayi, S., Abiola, B., Abdusalam, I., Morakinyo A. (2019). Biosynthesis, Characterisation and antimicrobial activity of gold nanoparticles from leaf extracts of *Annona muricata.* Journal of Nanostructure in Chemistry, 9(2), 111–117. DOI: 10.1007/s40097-019-0301-1

66. Hamad, K. M., Mahmoud, N. N., Al-Dabash, S., Al-Samad, L. A., Abdallah, M., & Al-Bakri, A. G. (2020). Fluconazole conjugated-gold nanorods as an antifungal nanomedicine with low cytotoxicity against human dermal fibroblasts. RSC Adv, 10, 25889-25897. DOI: 10.1039/ d0ra00297f

67. Lipovsky, A., Nitzan, Y., Gedanken, A., & Lubar, R. (2011). Antifungal activity of ZnO nanoparticles—the role of ROS mediated cell injury. Nanotechnology, 22, 105101.

68. Kim, S.W., Jung, J.H., Lamsal, K., Kim, Y. S., Min, J. S. & Lee, Y. S. (2012). Antifungal effects of silver nanoparticles (AgNPs) against various plant pathogenic fungi. Mycobiology 40(1), 53-58. DOI: 10.5941/MYCO.2012.40.1.053.

69. A. Jebali, Hajjar, F. H. E., Pourdanesh, F., Hekmatimoghaddam, S., Kazemi, B., Masoudi, A., Daliri, K., Sedighi., N. (2013). Silver and gold nanostructures: antifungal property of different shapes of these nanostructures on *Candida* species. Medical Mycology, 52(1), 65–72.
DOI: 10.3109/13693786.2013.822996

70. Eskandari-Nojedehi, M., Jafarizadeh-Malmiri, H., & Rahbar-Shahrouzi, J. (2018). Hydrothermal green synthesis of gold nanoparticles using mushroom (*Agaricus bisporus*) extract: physico-chemical characteristics and antifungal activity studies. Green Processing and Synthesis, 7(1), 38–47. DOI: 10.1515/gps-2017-0004

71. Chen, J., Wu, L., Lu, M., Lu, S., Li, Z., & Ding, W. (2020). Comparative Study on the Fungicidal Activity of Metallic MgO Nanoparticles and Macroscale MgO Against Soilborne Fungal Phytopathogens. Frontiers in Microbiology, 11, 365. DOI: 10.3389/fmicb.2020.00365

72. Rahimi, H., Roudbarmohammadi, S., Hamid Delavari, H., Roudbary, M. (2019). Antifungal effects of indolicidin-conjugated gold nanoparticles against fluconazole-resistant strains of Candida albicans isolated from patients with burn infection. International Journal of Nanomedicine, 14, 5323–5338. DOI: 10.2147/IJN.S207527.

Tables

Table 1. A comparison of antifungal activity of diverse nanomaterials with the GA-AuNC-NT

Nanomaterial tested	Parameters studied	Parameters studied in this present study	Significance of the present finding
Silver nanoparticles (Villamizar-Gallardo et al., 2016)	Fungicidal effect against *Fusarium solani* by solid and liquid assay No report of the molecular mechanism of antifungal activity Biocompatibility was not studied with the animal model	Highly stable gum acacia-gold nanocomposite fabricated natamycin was prepared by in situ green science principles. Antifungal activity against fungal strain *Aspergillus ochraceopealiformis* by studying growth inhibition parameters Measuring oxidative stress markers gene expression followed by determination of enzymatic and non-enzymatic antioxidants Biocompatibility was studied with the Wistar model	Enhancement of antifungal activity by inducing oxidative stress marker genes reveals the molecular mechanism of antifungal activity against *Aspergillus ochraceopealiformis* No toxic effect of the Wistar model reveals the best biocompatibility
Silver nanoparticles commercial formulation (Akpinar et al., 2021)	Fungal growth inhibition was studied. No report of the molecular mechanism of antifungal activity No report of biocompatibility	The effect of nanocomposite on the antifungal activity was studied by solid, liquid assays, mycelial fragmentation and spore germination inhibition assays Q RT-PCR studied relative gene expression of oxidative stress marker genes Changes in the enzymatic and non-enzymatic antioxidants were determined Animal toxicity studies using the Wistar model was carried out	Highly stable nano dimensional nanocomposite with potential antifungal activity was prepared via green science principles
Antifungal activity of ZnO nanoparticles against	The antifungal activity was studied by solid plate assay,	Growth inhibition studies by solid plate, liquid assay, mycelial fragmentation, spore germination assays,	The potential antifungal activity of the nanocomposite that

Penicillium (Zhang et al., 2019)	evaluated antioxidants enzymes status No report of the molecular mechanism of antifungal activity Biocompatibility was not studied with the animal model	Studied various enzymatic antioxidants, non-enzymatic antioxidant status Quantitative measurement of major oxidative stress markers gene expression Biocompatibility assessment was done with the animal model	synthesized via green science principles was determined from its distinct growth inhibition efficacy Induced ROS generation followed by triggering enzymatic and non-enzymatic antioxidants Quantified oxidative stress markers genes which reveal the molecular mechanism of antifungal activity No sign of toxic effect with the Wistar model demonstrates the best biocompatibility
Biologically synthesized gold nanoparticles against plant pathogenic fungi (Basu et al., 2018)	Studied antifungal activity by solid plate assay, spore germination inhibition assay No report of the molecular mechanism of antifungal activity Biocompatibility was not studied with the animal model	Antifungal activity was studied by solid, liquid assays, mycelial fragmentation and spore germination inhibition assays Q RT-PCR studied relative gene expression of oxidative stress marker genes Changes in the enzymatic and non-enzymatic antioxidants were determined Animal toxicity studies using the Wistar model was carried out	The first report of relative gene expression of oxidative stress markers, controlled or sustained release pattern, biocompatibility determination

Gold nanoparticles and titanium dioxide nanoparticles based antifungal activity against *candida albicans* (Rahimzadeh Torabi and Doudi, 2016)	A commercial formulation of AuNps tested against *C. albicans* by solid and liquid assays No report of the molecular mechanism of antifungal activity Biocompatibility was not studied with the animal model	Primary confirmation of antifungal activity by solid, liquid assays, fungal hyphae fragmentation, spore germination inhibition assays Quantitative expression profile of oxidative stress marker genes Release pattern using different solvents Biocompatibility using Wistar model	Oxidative stress-induced molecular mechanism reveals potential antifungal activity Effect of solvents on the controlled or sustained release of natamycin None of the toxic effects in the animal model suggests the potential biosafety
Fungicidal effect of gold nanoparticles (Folorunso et al., 2019)	A commercial formulation of AuNps tested against *C. albicans* by solid and liquid assays No report of the molecular mechanism of antifungal activity Biocompatibility was not studied with the animal model	Antifungal activity was studied by solid, liquid assays, mycelial fragmentation and spore germination inhibition assays Q RT-PCR studied relative gene expression of oxidative stress marker genes Changes in the enzymatic and non-enzymatic antioxidants were determined Animal toxicity studies using the Wistar model was carried out	The first report of relative gene expression of oxidative stress markers, controlled or sustained release pattern, biocompatibility determination
Fluoconazole doped gold nanorods (Hamad et al., 2020)	Growth inhibition of *candida albicans* and non-target effect against human dermal fibroblast	Survival limiting factors were studied by evaluating oxidative stress marker genes Wister model was used to determine the non-target effect	Confirmation of antifungal activity by effective induction of oxidative stress reveals the molecular

	No report of the molecular mechanism of antifungal activity Biocompatibility was not studied with the animal model		mechanism of antifungal activity Animal model studies demonstrate the biosafety
ZnO nanoparticles based antifungal activity (Lipovsky et al., 2011)	Determination of growth curve, survival rate parameters No report of the molecular mechanism of antifungal activity Biocompatibility was not studied with the animal model	Primary confirmation of antifungal activity by solid, liquid assays, fungal hyphae fragmentation, spore germination inhibition assays Quantitative expression profile of oxidative stress marker genes Release pattern using different solvents Biocompatibility using a Wistar model	Oxidative stress-induced molecular mechanism reveals potential antifungal activity. Effect of solvents on the controlled or sustained release of natamycin None of the toxic effects in the animal model suggests the potential biosafety
Phyto mediated gold nanoparticles (Kim et al., 2012)	Agar diffusion assay was used to determine antifungal activity No report of the molecular mechanism of antifungal activity Biocompatibility was not studied with the animal model	Antifungal activity was studied by solid, liquid assays, mycelial fragmentation and spore germination inhibition assays Q RT-PCR studied relative gene expression of oxidative stress marker genes Changes in the enzymatic and non-enzymatic antioxidants were determined. Animal toxicity studies using the Wistar model was carried out	The first report of relative gene expression of oxidative stress markers, controlled or sustained release pattern, biocompatibility determination
Silver	Growth	Growth inhibition studies by	The first report of

nanoparticles against plant pathogenic fungi (Jebali et al., 2013)	inhibition assay No report of the molecular mechanism of antifungal activity Biocompatibility was not studied with the animal model	solid plate, liquid assay, mycelial fragmentation, spore germination assays, Studied various enzymatic antioxidants, non-enzymatic antioxidant status Quantitative measurement of major oxidative stress markers gene expression. A biocompatibility assessment was done with the animal model	relative gene expression of oxidative stress markers, controlled or sustained release pattern, biocompatibility determination
The antifungal activity of silver and gold nanostructures (Eskandari-Nojedehi et al., 2018)	Micro dilution agar diffusion assays were carried out No report of the molecular mechanism of antifungal activity Biocompatibility was not studied with the animal model	The antifungal activity was studied by solid, liquid assays, mycelial fragmentation and spore germination inhibition assays Q RT-PCR studied relative gene expression of oxidative stress marker genes Changes in the enzymatic and non-enzymatic antioxidants were determined Animal toxicity studies using the Wistar model was carried out	Confirmation of antifungal activity by effective induction of oxidative stress reveals the molecular mechanism of antifungal activity Animal model studies demonstrate the biosafety
Biologically synthesized gold nanoparticles (Chen et al., 2020)	Well diffusion assay was adopted No report of the molecular mechanism of antifungal activity Biocompatibility was not studied with the animal model	Primary confirmation of antifungal activity by solid, liquid assays, fungal hyphae fragmentation, spore germination inhibition assays. Quantitative expression profile of oxidative stress marker genes Release pattern using different solvents	The first report of relative gene expression of oxidative stress markers, controlled or sustained release pattern, biocompatibility determination

		Biocompatibility using a Wistar rat model	
MgO nanoparticles against soil-borne phytopathogens (Rahimi et al., 2019)	Fungal growth measurements, antioxidants status evaluation No report of the molecular mechanism of antifungal activity Biocompatibility was not studied with the animal model	Growth inhibition studies by solid plate, liquid assay, mycelial fragmentation, spore germination assays, Studied various enzymatic antioxidants, non-enzymatic antioxidant status Quantitative measurement of major oxidative stress markers gene expression Biocompatibility assessment was done with the animal model	The first report of relative gene expression of oxidative stress markers, controlled or sustained release pattern, biocompatibility determination

Table 2. Effect of nanocomposite packaging on fungal colony count

Treatment	Colony-forming units/gram		
	10^{th} day	20^{th} day	30^{th} day
Control	$67.2 X10^{4}$ [a]	$82X10^{4}$ [a]	$81.3X19^{5}$ [a]
Nanocomposite	0.0	0.0	0.0

[a] Column carries alphabet is statistically significant at 0.01 % level by DMRT

Figures

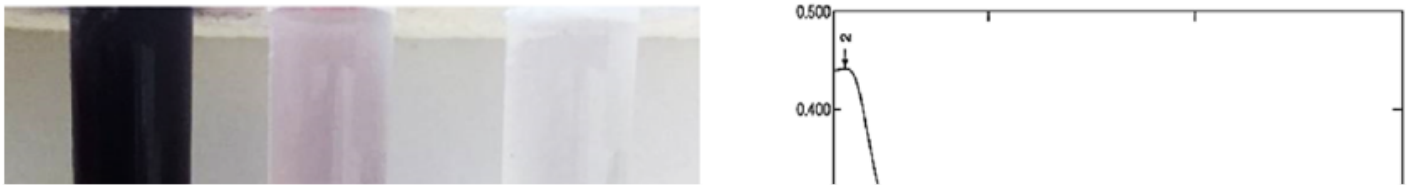

Figure 1

(a) Reaction mixture (A) AuNps (B) GA-AiNC- NT (C) GA-NT mixture (b) UV- visible spectra of free AuNps (c) UV- visible spectra of GA-AuNC-NT (merged with free AuNps)

Figure 2

FTIR spectra (a) Natamycin (b) AuNps (c) Gum acacia (d) Nanocomposite (GA-AuNC-NT)

Figure 3

Characterization of the nanocomposite (a)- 2D, ED AFM micrograph (b) Particles size distribution pattern (c) SEM micrograph (d) thermogravimetric analysis (TGA)

Figure 4

Phylogenetic tree of *Aspergillus ochraceopealiformis*

Figure 5

Effect of nanocomposite on the growth inhibition (a) and biomass dry weight of *Aspergillus ochraceopealiformis*

Figure 6

Anti fungal activity- Microscopic examination of fungal hyphae fragmentation (a) Control (b) GA (c) AuNps (d) GA-AuNC- NT (e)Fungal fragmentation percentage

Figure 7

Fig 7. Microscopic examination of spore germination (a) Control (b) GA (c) AuNps (d) GA-AuNC-NT (e) spore germination percentage

Fig 7 (i). SEM micrograph of fungal vegetative and reproductive structure

(a) Control (b) 25

Fig 7 (ii). SEM micrograph of fungal vegetative and reproductive structure

Figure 8

Reactive oxygen species (ROS) generation in *Aspergillus ochraceopealiformis*

Figure 9

cDNA expression of oxidative stress genes (A) – CAT gene- Lane 1- Free AuNps,lane 2-nanocomposite,lane 3-gum acacia, lane 4-free natamycin,lane 5- control

(B) SOD- lane 1- control, lane 2- nanocomposite,lane 3-free AuNp,lane 4-free natamycin,lane5- gum acacia

(C) POD –lane 1- control.lane 2-free natamycin,lane 3-nanocomposite,lane 4- free AuNp,lane 5-gum acacia

Figure 10

Relative gene expression of oxidative stress marker genes (a) CAT (b) SOD (c) POD

Figure 11

Enzymatic and non enzymatic anti oxidants status of *Aspergillus ochraceopealiformis*

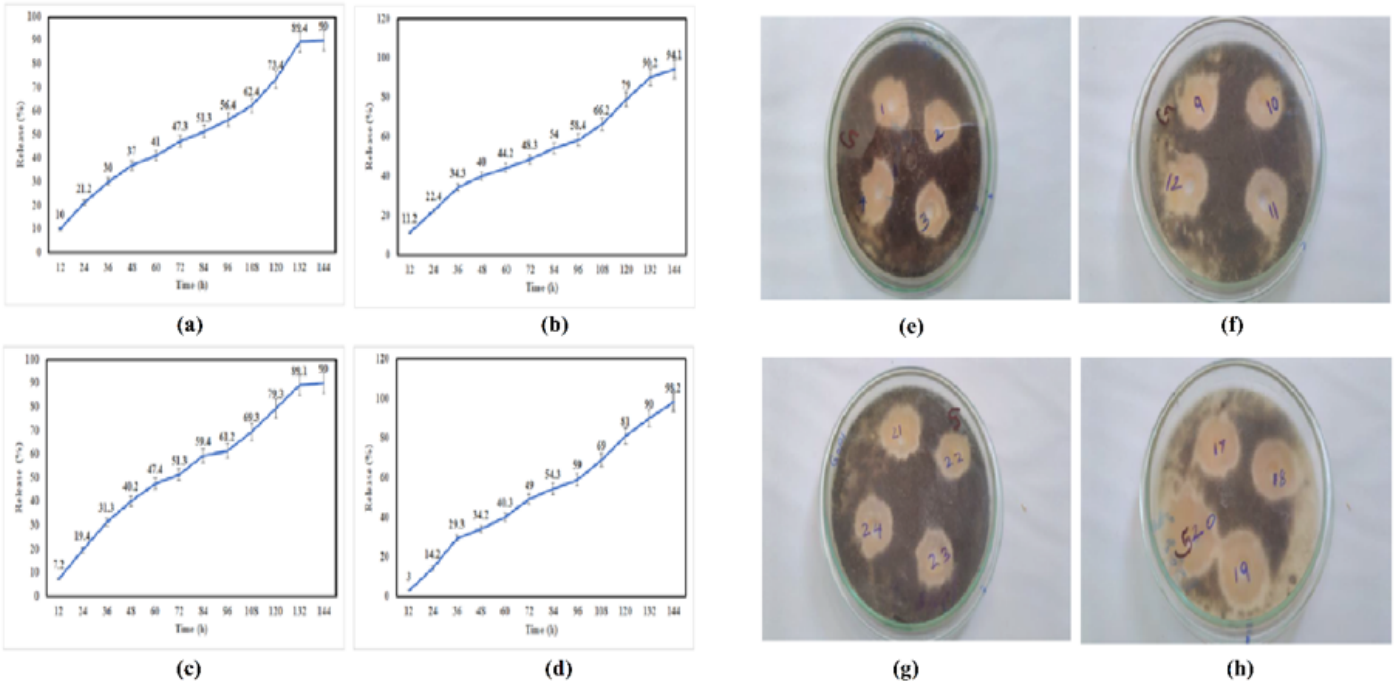

Figure 12

The effect of solvents on the release of natamycin from the synthesised nanocomposite ((a) Zone of inhibition of released NT against the tested fungal strain e- distilled water,b-ethanol (c)acetone (d) Phosphate buffered saline

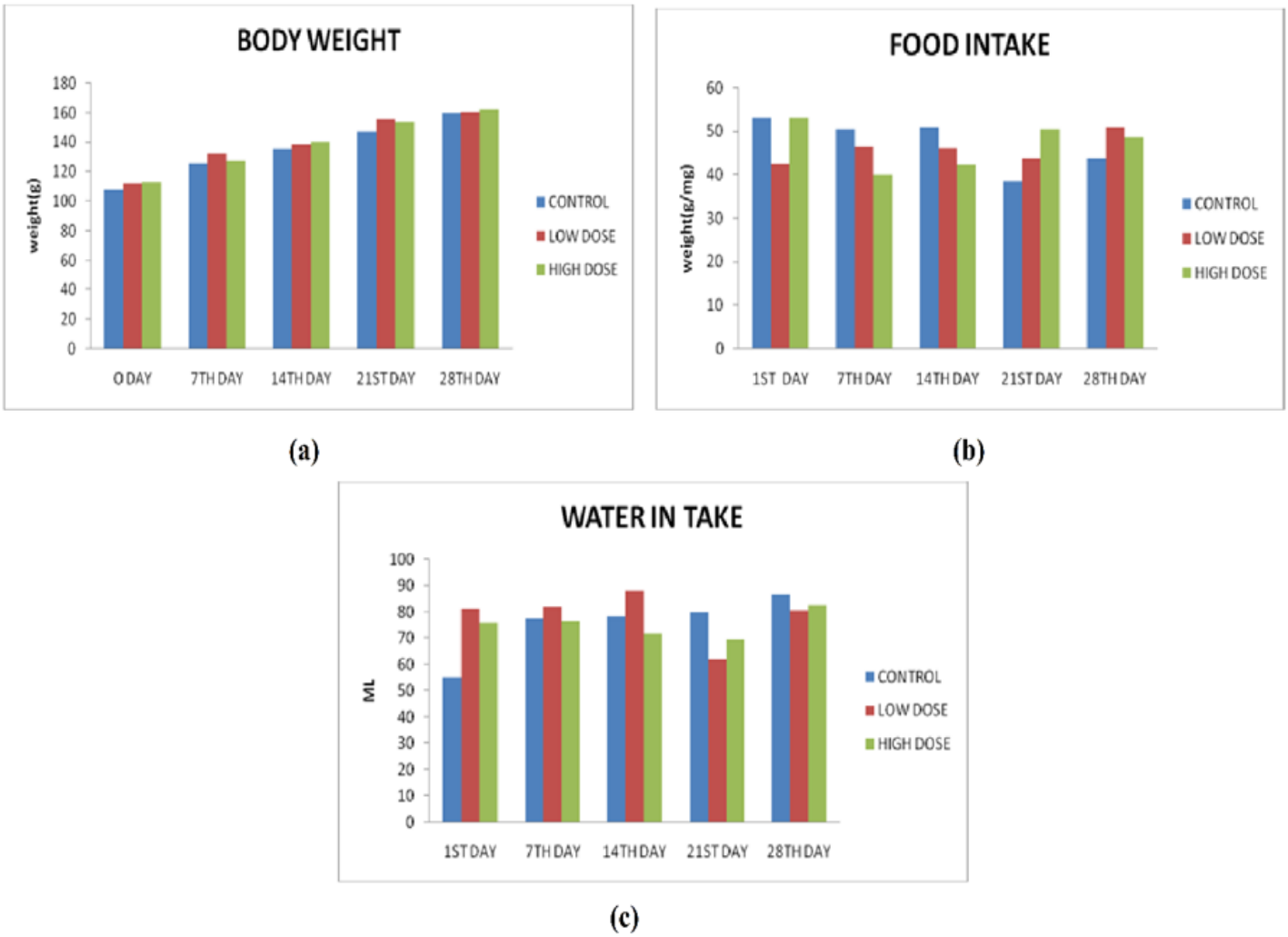

Figure 13

Effect of Nanocomposite on the bodyweight (a) food intake (c) water intake of Wistar Rat model

Figure 14

Effect of nanocomposite on organ weights (a-f) liver function markers (g-i),lipid profile (j-l)

Figure 15

Effect of nanocomposite on kidney function parameters (a-c), hematological parameters (d-g)

Figure 16

Histopathological examination. myocardium of Wistar Rat model (a) Control (b) Low dosage group (c) High dosage group (d) Liver- Control (e) Low dosage group (f) High dosage group. (g) Liver Control (b) Low dosage group (i) High dosage group, Kidney - (j) Control (k) Low dosage group (l) High dosage group

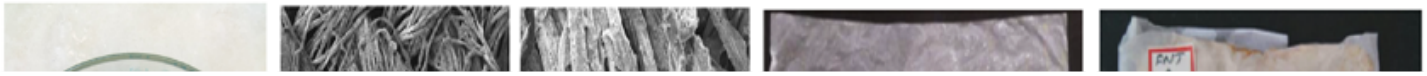

Figure 17

Nanocomposite coating (a) zone of inhibition nanocomposite with blender for coating, b- SEM micrograph of un coated packaged material , c- Effect of nanocomposite packaging on the proximate composition of bread (d) Effect of nanocomposite on the anti oxidative enzymes status (e) Nanocomposite coated packaging material (f (Control (h) free natamycin coated packing (i) nanocomposite coated packing

Figure 18

Effect of nanocomposite on proximate composition (a) anti oxidative activity (b) of nanocomposite coated packed breads.

Supplementary Files

This is a list of supplementary files associated with this preprint. Click to download.

- Onlinefloatimage1.png